The vicinity of the galactic supergiant B[e] star CPD−57° 2874 from near- and mid-IR long baseline spectro-interferometry with the VLTI (AMBER and MIDI)

A. Domiciano de Souza[1], T. Driebe[1], O. Chesneau[2], K.-H. Hofmann[1], S. Kraus[1], A. S. Miroshnichenko[1,3], K. Ohnaka[1], R. G. Petrov[4], Th. Preibisch[1], P. Stee[2], G. Weigelt[1]

[1] *Max-Planck-Institut für Radioastronomie, Auf dem Hügel 69, 53121 Bonn, Germany*

[2] *Observatoire de la Côte d'Azur, Gemini, CNRS UMR 6203, Avenue Copernic, 06130 Grasse, France*

[3] *Dept. of Physics and Astronomy, P.O. Box 26170, University of North Carolina at Greensboro, Greensboro, NC 27402–6170, USA*

[4] *Laboratoire Universitaire d'Astrophysique de Nice (LUAN), CNRS UMR 6525, UNSA, Parc Valrose, 06108 Nice, France*

Abstract. We present the first spectro-interferometric observations of the circumstellar envelope (CSE) of a B[e] supergiant (CPD−57° 2874), performed with the Very Large Telescope Interferometer (VLTI) using the beam-combiner instruments AMBER (near-IR interferometry with three 8.3 m Unit Telescopes or UTs) and MIDI (mid-IR interferometry with two UTs). Our observations of the CSE are well fitted by an elliptical Gaussian model with FWHM diameters varying linearly with wavelength. Typical diameters measured are $\simeq 1.8 \times 3.4$ mas or $\simeq 4.5 \times 8.5$ AU (adopting a distance of 2.5 kpc) at $2.2\,\mu$m, and $\simeq 12 \times 15$ mas or $\simeq 30 \times 38$ AU at $12\,\mu$m. We show that a spherical dust model reproduces the SED but it underestimates the MIDI visibilities, suggesting that a dense equatorial disk is required to account for the compact dust-emitting region observed. Moreover, the derived major-axis position angle in the mid-IR ($\simeq 144°$) agrees well with previous polarimetric data, hinting that the hot-dust emission originates in a disk-like structure. Our results support the non-spherical CSE paradigm for B[e] supergiants.

1. Introduction

CPD−57° 2874 is a poorly-studied object, for which McGregor et al. (1988) suggested a distance of $d = 2.5$ kpc, assuming that it belongs to the Carina OB association. A high reddening and the presence of CO emission bands at $2.3 - 2.4\,\mu$m makes it compatible with the supergiant B[e] (sgB[e]) class. Zickgraf (2003) obtained high-resolution optical spectra exhibiting double-peaked emission lines that are suggestive of a flattened CSE geometry, typical for sgB[e] stars. However, the physical parameters of neither the star nor its CSE have been studied in detail yet.

1

2. Results

We report here our results on CPD$-57°\,2874$ based on recent (Dec/2004 - Feb/2005) spectro-interferometric observations performed with the VLTI instruments AMBER (e.g., Petrov et al. 2003) and MIDI (e.g., Leinert et al. 2004).

Figures 1 and 2 show the spectra and visibilities obtained with AMBER and MIDI, respectively. CPD$-57°\,2874$ is resolved in both spectral regions at all projected baselines B_p and position angles PA. As a zero-order size estimate these figures also show the uniform disk angular diameters θ_UD obtained from the visibilities at each spectral channel. Figure 3 (left) shows the θ_UD as a function of the baseline position angle observed with AMBER and MIDI. The measured sizes are clearly different on the 4 spectral channels chosen ($2.2\,\mu$m, Brγ line, $7.9\,\mu$m, and $12.1\,\mu$m); in particular, the mid-IR sizes are much larger than those in the near-IR. Indications of a flattened CSE is more evident in the near-IR than in the mid-IR but, as we will show in Sect. 3., both AMBER and MIDI observations suggest a non-spherical CSE.

The AMBER observations show a zero closure phase (Fig. 3 right) at all wavelengths (within the noise level of a few degrees). This is a strong indication that the near-IR emitting regions (continuum and Brγ line) have an approximately centrally-symmetric intensity distribution.

Since sgB[e] stars are thought to have non-spherical winds, we expect an elongated shape for their CSE, unless the star is seen close to pole-on. Hereafter, we show that both AMBER and MIDI observations can indeed be well reproduced by an elliptical Gaussian model for the CSE intensity distribution, corresponding to visibilities of the form:

$$V(u,v) = \exp\left\{\frac{-\pi^2(2a)^2}{4\ln 2}[u^2 + (Dv)^2]\right\} \tag{1}$$

where u and v are the spatial-frequency coordinates, $2a$ is the major-axis FWHM of the intensity distribution (image plane), and D is the ratio between the minor and major axes FWHM ($D = 2b/2a$). Since, in general, $2a$ forms an angle α with the North direction (towards the East), u and v should be replaced in Eq. 1 by $(u\sin\alpha + v\cos\alpha)$ and $(u\cos\alpha - v\sin\alpha)$, respectively. A preliminary analysis of V at each individual λ showed that D and α can be considered independent on λ within a given spectral band (K or N). On the other hand, the size varies with λ, as one can see from the $\theta_\mathrm{UD}(\lambda)$ curves in Figs. 1 to 3.

2.1. Size and geometry in the K band

We interpret the AMBER observations in terms of an elliptical Gaussian model (Eq. 1) with a chromatic variation of the size. The $\theta_\mathrm{UD}(\lambda)$ curves in Fig. 1 suggest a linear increase of the size within this part of the K band. In addition, the AMBER visibilities decrease significantly inside Brγ, indicating that the line-forming region is more extended than the region responsible for the underlying continuum. Based on these considerations, we adopted the following expression for the major-axis FWHM:

$$2a(\lambda) = 2a_0 + C_1(\lambda - \lambda_0) + C_2\exp\left[-4\ln 2\left(\frac{\lambda - \lambda_\mathrm{Br\gamma}}{\Delta\lambda}\right)^2\right] \tag{2}$$

Table 1. Model parameters and χ^2_{red} (reduced chi-squared) derived from the fit of an elliptical Gaussian (Eqs. 1 and 2) to the VLTI/AMBER and VLTI/MIDI visibilities. Angular sizes (in mas) correspond to FWHM diameters. The errors on the fit parameters are dominated by the calibration errors of the instrumental transfer function, derived from the calibrator stars.

Parameter	AMBER	MIDI ($< 10\,\mu$m)	MIDI ($> 10\,\mu$m)
λ_0 (μm)	2.2	8.0	12.0
major axis $2\,a_0$ (mas)	3.4 ± 0.2	10.1 ± 0.7	15.3 ± 0.7
C_1 (mas/μm)	1.99 ± 0.24	2.58 ± 0.41	0.45 ± 0.22
position angle α (°)	$173° \pm 9°$	$145° \pm 6°$	$143° \pm 6°$
$D = 2b/2a$	0.53 ± 0.03	0.76 ± 0.11	0.80 ± 0.10
minor axis $2\,b_0$ (mas)	1.8 ± 0.1	7.7 ± 1.0	12.2 ± 1.1
Brγ: C_2 (mas)	1.2 ± 0.1	–	–
Brγ: $\Delta\lambda$ ($10^{-3}\,\mu$m)	1.8 ± 0.2	–	–
χ^2_{red}	0.7	0.1	0.1

where $2a_0$ is the major-axis FWHM at a chosen reference wavelength $\lambda_0 (= 2.2\,\mu$m), and C_1 is the slope of $2a(\lambda)$. The size increase within Brγ is modelled by a Gaussian with an amplitude C_2 and FWHM $\Delta\lambda$, centered at $\lambda_{\mathrm{Br}\gamma} = 2.165\,\mu$m. Figure 1 shows a rather good fit of this model to the observed visibilities both in the continuum and inside Brγ. The parameters derived from the fit are listed in Table 1.

2.2. Size and geometry in the N band

Similarly to the analysis of the AMBER visibilities, we interpret the MIDI observations of CPD$-57°\,2874$ in terms of an elliptical Gaussian model (Eq. 1) with a size varying linearly with λ as given in Eq. 2 (for the analysis of the MIDI data the parameter C_2 is set to zero). Additionally, since θ_{UD} shows a stronger λ-dependence between 7.9 and 9.8 μm compared to the region between 10.2 and 13.5 μm (see Fig. 2), we performed an independent fit for each of these two spectral regions. This elliptical Gaussian model provides a good fit to the MIDI visibilities as also shown in Fig. 2. The parameters corresponding to the fit in the two spectral regions within the N band are listed in Table 1.

3. Discussion and conclusions

To further investigate the geometry of the CSE, we attempted to simultaneously fit the MIDI visibilities and the spectral energy distribution (SED) using the spherical 1D code DUSTY (Ivezić & Elitzur 1997). To reproduce the featureless spectrum around $10\,\mu$m, we used large silicate grains and/or carbonaceous dust. The nature of the dust and the featureless mid-IR spectrum will be addressed in detail elsewhere. This spherical model in the optically-thin regime can nicely fit the SED (as shown in Fig. 4), but it significantly underestimates the mid-IR visibilities, even when the model parameters are varied considerably. This means that the measured dust-emitting region is too compact ($2a \sim 10-16$ mas

4

or $25 - 40$ AU; see Table 1) to be reproduced by a spherical model (even though the SED fit is acceptable). Only a disk-like structure seems to allow the dust to survive within ~ 10 AU from the star (see Kraus & Lamers 2003).

Another argument against a spherical CSE comes from polarization measurements of Yudin & Evans (1998). After correction for the interstellar polarization, Yudin (private communication) estimated an intrinsic polarization position angle $\simeq 45° - 55°$. Interestingly, within the error bars this angle is perpendicular to the major-axis PA we derived from the MIDI data ($\alpha \simeq 144°$; see Table 1), as is expected from a disk-like dusty CSE.

Thanks to the unprecedent combination of interferometric resolution, multispectral wavelength coverage and relatively high spectral resolution now available from the VLTI we measured the size and geometry of the CSE of a sgB[e] star in the near- and mid-IR. We hope that the present work will open the door for new spectro-interferometric observations of these complex and intriguing objects as well as motivate the development of interferometry-oriented and physically-consistent models for such objects. A more complete description of the present work is given by Domiciano de Souza et al. (2005).

References

Domiciano de Souza, A., Driebe, T., Chesneau, O., et al. 2005, A&A, accepted
Drilling, J. S. 1991, ApJS, 76, 1033
Egan, M. P., Price, S. D., Kraemer, K. E., et al. 2003, The Midcourse Space Experiment Point Source Catalog (v.2.3)
Ivezić, Ž., & Elitzur, M. 1997, MNRAS, 287, 799
Joint IRAS Science Working Group 1988, Point Source Catalog
Kraus, M., & Lamers, H. J. G. L. M. 2003, A&A, 405, 165
Leinert, Ch., van Boekel, R., Waters, L.B.F.M., et al. 2004, A&A, 423, 537
McGregor, P. J., Hyland, A. R., & Hillier, D. J. 1988, ApJ, 324, 1071
Petrov, R. G., Malbet, F., Weigelt, G., et al. 2003, SPIE proc., 4838, 924
Sloan, G. C., Kraemer, K. E., Price, S. D., & Shipman, R. F. 2003, ApJS, 147, 379
Yudin, R. V., & Evans, A. 1998, A&AS, 131, 401
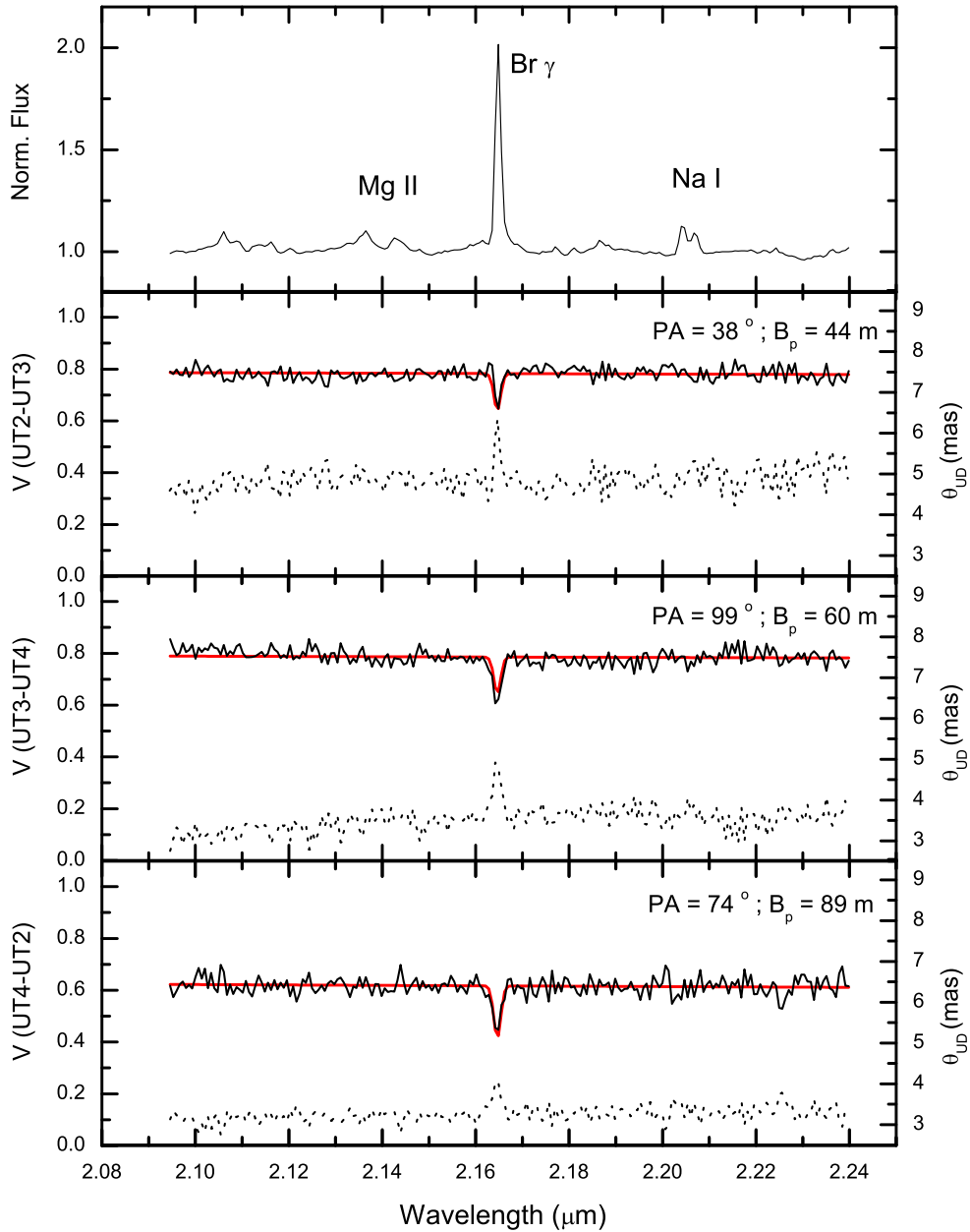Zickgraf, F.-J. 2003, A&A, 408, 257

Figure 1.   VLTI/AMBER observations of CPD−57° 2874 obtained around
Brγ with spectral resolution $R = 1500$. The normalized flux is shown in
the top panel and the visibilities V for each baseline are given in the other
panels (the corresponding projected baselines B_p and position angles PA are
indicated). The errors in V are $\simeq \pm 5\%$. The dotted lines are the uniform disk
angular diameters θ_{UD} in mas (to be read from the scales on the right axis),
computed from V at each λ as a zero-order size estimate. The visibilities
obtained from the elliptical Gaussian model fits the observations quite well
(smooth solid lines; Eqs. 1 and 2, and Table 1). In contrast to the Brγ line,
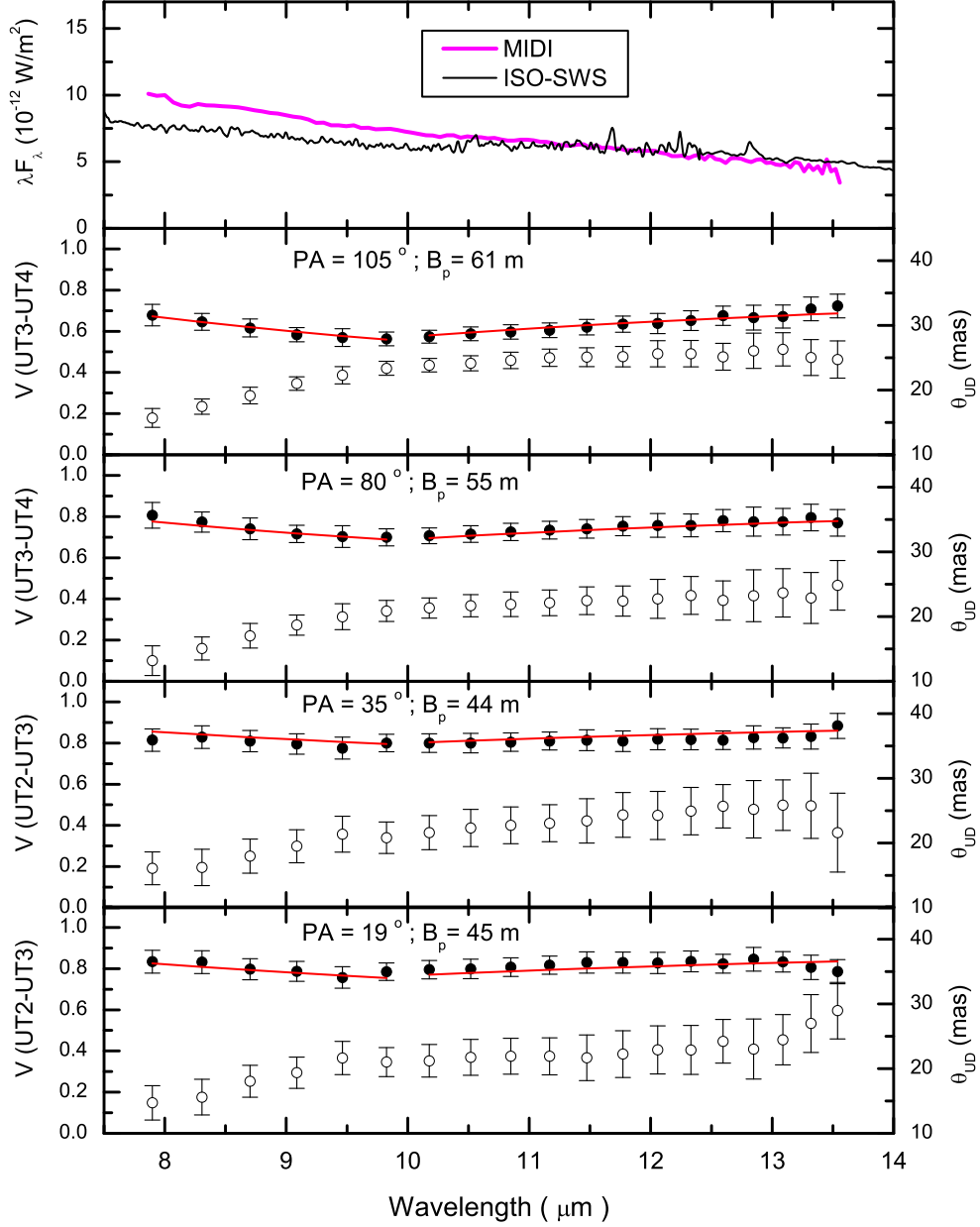the Mg II and Na I lines do not show any clear signature on the visibilities.

Figure 2.   VLTI/MIDI observations of CPD−57° 2874 obtained in the mid-IR with spectral resolution $R = 30$. V and $\theta_{\rm UD}$ are shown as filled and open circles, respectively. The MIDI and ISO-SWS (Sloan et al. 2003) spectra (top panel) show no clear evidence of a silicate feature around $10\,\mu$m. The MIDI visibilities are well fitted with an elliptical Gaussian model (solid lines; Eqs. 1 and 2, and Table 1).
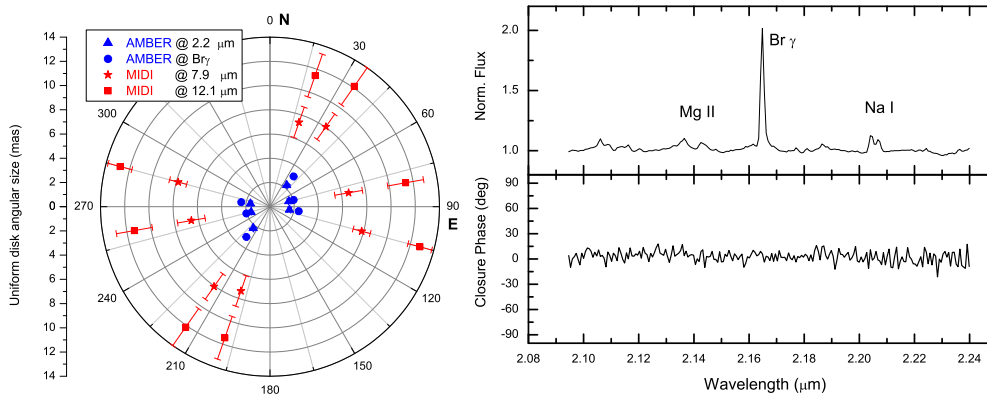
Figure 3.   *Left:* Uniform disk sizes dependence on the baseline position angle (in degrees) for 2 selected wavelengths both from AMBER (continuum at $2.2\,\mu$m and center of the Brγ line) and from MIDI ($7.9\,\mu$m and $12.1\,\mu$m). The central star is supposed to be at the center of the plot and the distance between 2 symmetrical points gives the corresponding uniform disk angular diameter ($\theta_{\rm UD}$) of the CSE. The error bars on the AMBER $\theta_{\rm UD}$ have similar sizes as their corresponding symbols. Although the $\theta_{\rm UD}$ is a zero-order estimate, this figure allows us to directly compare the CSE sizes in the near- and mid-IR. *Right:* VLTI/AMBER closure phase for CPD$-57°\,2874$ obtained around Brγ with $R = 1500$. Within the noise level ($\simeq \pm10°$) the closure phase is zero (continuum and Brγ line) suggesting a centrally-symmetric intensity distribution in the near-IR. Spherical and non-spherical (with axial-symmetry) CSEs are thus compatible with the zero closure phase measured with AMBER.
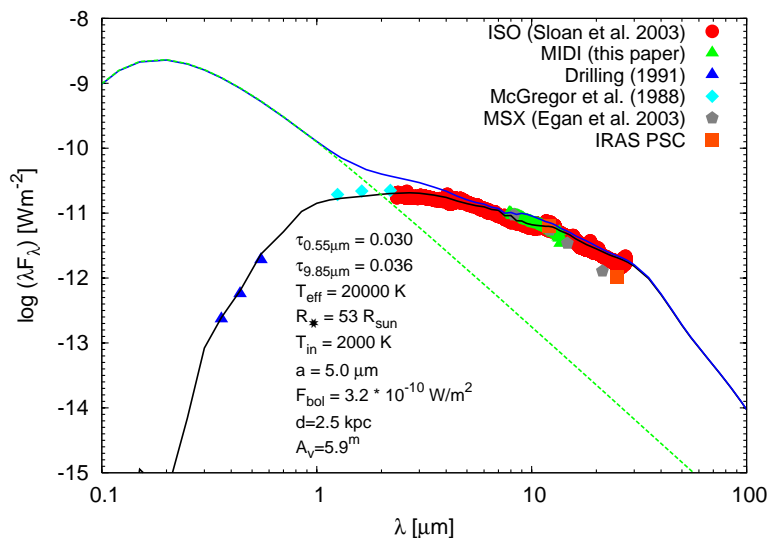

Figure 4.   The SED of CPD$-57°\,2874$ constructed from several sources (see figure label). The solid lines are the observed and dereddened SEDs modelled with the code DUSTY (Ivezić & Elitzur 1997), while the dashed line indicates the assumed blackbody spectrum of the central star. The parameters adopted for this model are listed in the figure: $T_{\rm in}$ is the temperature at the inner dust shell boundary, a is the diameter of the silicate grains, and the other symbols have their usual meanings. A standard r^{-2} dust-density law was assumed.